JOURNAL OF THE KOREAN ASTRONOMICAL SOCIETY
34: 59~66, 2001

ULTRAVIOLET ISOPHOTE SHAPES OF NEARBY ELLIPTICAL GALAXIES AND SPIRAL BULGES

YOUNG-JONG SOHN
Center for Space Astrophysics, Yonsei University, Seoul 120-749, Korea
E-mail: sohnyj@csa.yonsei.ac.kr
(Received May 28, 2001; accepted Jul. 18, 2001)

ABSTRACT

In this paper, we investigate the correlation between the radial ultraviolet color distribution and the shapes of the ultraviolet isophote for elliptical galaxies (M32, NGC 1399) and spiral bulges (of M31, M81) by using their archival *UIT* images. For M31, M81, and NGC 1399, the radial ultraviolet color distributions show a two-component trend; as the distance from the galactic center increase the color becomes redder in the inner region while it becomes bluer in the outer region. On the other hand, the color of M32 continues to become bluer with the increasing galactocentric distance. We also find, unlike the optical/IR images, significant variations of the position angle and the ellipticity in the ultraviolet isophotes of M31, M81, and NGC 1399 through the inner regions. For M32, the variation is significant in the outer region. Since these variation implies the triaxiality of their intrinsic shapes, we suggest that the early-type galaxies and spiral bulges with a radial color gradient in ultraviolet tend to have a triaxiality. On the other hand, the shape parameter characterized by the fourth order cosine Fourier coefficient of the isophote, $a(4)/a$, indicates that the systematic deviations of the ultraviolet isophotes of the four galaxies are smaller than ~0.2% in units of the semi-major axis. The latter result implies that the ultraviolet isophotes of the galaxies have a pure elliptical shape rather than the boxy or disky shapes. Therefore, there is no clear evidence of correlation between the radial ultraviolet color gradient and the boxy/disky shapes of isophotes.

Key words: galaxies: individual (M31, M32, M81, NGC1399) - galaxies: structure - ultraviolet: general

I. INTRODUCTION

Ultraviolet (UV) observations of elliptical galaxies and spiral bulges offer an important means of understanding evolution of hot stellar populations in the systems and the galaxy formation and evolution. The balloon/rocket-borne experiments and space telescopes flown on satellites have derived several distinctive UV characteristics in the systems (O'Connell 1999). One of the most important finding is the UV excess (UVX) phenomenon of these systems, which was first discovered from the observation of some nearby ellipticals and the central bulge of the M31 by using the detector mounted on *OAO*-2 satellite (Code 1969; Code & Welch 1979). Before these observations, appreciable number of stars hotter than their main sequence turnoffs was not expected. To date, UVX has been found in many normal ellipticals and bulges of spiral galaxies. The strength of UVX varies considerably by about 2~3 mag in FUV-V colors (e.g., Burstein et al. 1988; Dorman, O'Connell & Rood 1995). Candidates of hot UV-bright stellar objects include massive *OB* stars, low-mass stars in advanced stage of stellar evolution, and low-mass products of binary interactions. Recent observational and theoretical evidences show that the main component responsible for the strong UV emission is the old population of these systems, i.e., the low-mass, small-envelope, helium-burning stars in horizontal branch and subsequent phase of evolution (see O'Connell 1999 for review).

From the photometry of the *UIT* images obtained by using 1990 Astro-1 mission, O'Connell et al. (1992) found strong radial gradients in FUV-NUV color for two ellipticals (M32, NGC 1399) and bulges of two spiral galaxies (M31, M81). They found that the UVX became stronger as the galactocentric distance decreases for three galaxies (i.e., M31, M81, and NGC 1399), implying the possibility that a hot UV population is more strongly concentrated at the center of the galaxies. On the other hands, they found M32 exhibited a large reversed gradient, may be caused by the age gradient, where the stars in the central regions are tend to be younger.

Ohl et al. (1998) presented the FUV (1500 Å) surface brightness and FUV-B color profiles for 8 E/S0 galaxies by using the images taken with the *UIT* during the

Astro-2 mission. They found that the radial FUV profiles of 3 galaxies (M60, M49, and NGC 3379) were more consistent with an exponential function than $r^{1/4}$ de Vaucouleurs law, while the *B*-band profiles of all eight objects were well fitted by de Vaucouleurs law. The FUV-*B* color became redder with increasing r in all cases except M32, implying that the FUV light is more concentrated at the galaxy center than in the optical band. However, they found no correlation between the gradient in the FUV-*B* color and metallicity based on Mg absorption features, suggesting that metallicity is not the sole parameter controlling the UVX component in old populations.

Several evidences have been presented on the correlations of the UVX to other properties of the elliptical galaxies and spiral bulges. Metal abundance and age differences are the two simplest explanations of the UVX variations (Burstein et al. 1988; Lee 1994; Park & Lee 1997). It was proposed that the UV output might also be affected by other properties coupled with metallicity and age, such as mass loss processes on the RGB and the helium abundance of the UVX populations (e.g., Greggio & Renzini 1990; Chiosi 1996; Yi, Demarque, & Oemler 1997). More interestingly, Longo et al. (1989) and Bender & Möllenhoff (1987) mentioned that ellipticals with stronger UVX components are more likely to have boxy isophotal shapes. Observational (Nieto 1989; Bender 1988) and theoretical works (Binney & Petrou 1985; May, van Albada, & Norman 1985) proposed the possibility that boxy isophotes can be produced by the galactic interaction and merger. It is, therefore, possible that the UVX is influenced by the dynamical environment of galaxies.

On the other hand, there has been very few attempts to investigate the dependence of the UVX on galaxy morphology in the UV isophote (cf. O'Connell 1999, Kuchinski et al. 2000). The UV surface photometries performed by O'Connell et al. (1992) and Ohl et al. (1998) were based on the simple circular annuli photometry to the NUV and FUV images of the galaxies, and thus their results do not provide information about the correlation between the UV isophote morphologies and the radial UVX gradient.

In this paper, we report the results of the UV surface photometry based on the more sophiscated ellipse fitting to the NUV and FUV images of nearby ellipticals (M32 and NGC 1399) and spiral bulges (M31 and M81) obtained from the *UIT* Astro-1 mission and examine the correlations between the radial gradient in the UVX and the isophote shape parameters of the sample galaxies.

The paper is organized in the following way. In Section 2, we describe the details of the archival *UIT* data. In Section 3, we describe the UV surface photometry based on the ellipse fitting to the isophote and present the UV surface brightness and color profiles. In Section 3, we present the results of the isophote shape analysis including the radial variations of the position angle, ellipticity, and $a(4)/a$. In Section 4, we discuss the correlation between the radial UVX variation and the the shape parameters and the other properties. We summarize our findings in Section 5.

Table 1. UIT images used in this study

Target	Image number	Bandpass	Exposure time (s)
M31	nuv0236	A1	330
M31	fuv0266	B1	384
M32	nuv0388	A1	583
M32	fuv0485	B1	582
M81	nuv0442	A1	639
M81	fuv0556	B1	640
NGC 1399	nuv0216	A1	1099
NGC 1399	fuv0232	B1	1454

II. UIT DATA

The NUV and FUV images of the sample galaxies are obtained from the archival *UIT* data of Astro-1 mission in 1990. The *UIT* is a 38-cm Ritchey-Chrétien telescope with a focal ratio of 9.0 and a 40′ field of view. Stecher et al. (1992, 1997) described the *UIT* instrumentation and initial data reduction process, including digitization, linearization, flat-fielding, and geometric distortion corrections. Standard *UIT* data process produces several images at each stage of the batch data reduction procedures (Hill et al. 1993). Among them, we use the "north-up undistorted intensity" images. They have a 2048×2048 format and are resampled and rotated to north-up and east-left format with distortion removed. The resulting image scale is 11″.14 per pixel.

We select images with the deepest exposures in NUV A1 and FUV B1 filters. The FUV B1 and NUV A1 passbands are centered at 1520 Å and 2490 Å with widths 354 and 1150 Å, respectively. The exposure numbers, passbands, and exposure times of the images used in this investigation are listed in Table 1.

III. UV SURFACE PHOTOMETRY AND RESULTS

(a) Data Acquisition

We estimate the sky levels in NUV and FUV frames of each galaxy by measuring intensities in ~20 different positions away from the galaxy. We adopt the median value of these measurements as a sky level of each frame. Typical sky levels are μ_λ(1520 Å)>23.3 mag arc-

sec^{-2} and μ_λ(2490 Å)>24.5 mag arcsec^{-2}. In case of M32, however, the sky level is somewhat bright, i.e. μ_λ(1520 Å)~22.0 mag arcsec^{-2} and μ_λ(2490 Å)~24.0 mag arcsec^{-2} due to the contamination from the outer disk of M31. For the bulges of M31 and M81, there would be the exponential disk contribution to the background level. It is worth noting here that the *UIT* telescope used Kodak IIa-O film as its detector, which is not a linear device. Therefore the final intensity images of *UIT*, unlike those of CCDs, still have base level plate fog remaining. We note, however, that the UV surface brightness and color over the inner region of the galaxies are not strongly affected by the variation of background error up to ±0.7 mag (O'Connell et al. 1992). An error of ±0.7 mag in the level of background is actually error of nearly a factor of 2 in surface brightness, and most of the background errors are smaller than this in the UIT data. We should note, however, even an error of only 0.2 mag in background level is ~20% in background brightness. We, therefore, keep in mind the uncertainty caused by the irregular pattern of plate fog on films.

To fit ellipse to the isophotes of the sample galaxies, we use the ELLIPSE task in the ISOPHOT package (Busko 1996) which is a part of the external IRAF package STSDAS. In this process, we first determine the accurate position of the galaxy on the ~3" pixels median-filtered NUV image by applying the CENTER task in IRAF to the area around the visual center with a typical radius of 10~20 pixels. The center position is double checked by examining the corresponding contour maps and intensity profiles. We then mask out foreground stars and any artifacts on the images before the ellipse fitting. The ellipse center is fixed, and the ellipticity and the position angle are then determined by running the ELLIPSE task on the NUV frame of each galaxy. Ellipse fitting is done at a number of discrete radii with a step of 5 pixels (corresponding to 5".7) to diminish the crowding effect caused by the typical ~3" FWHM of most *UIT* frames. The ellipse parameters derived on the NUV frame are then used to obtain the surface brightness profiles of FUV image of the galaxy. The ellipse fitting was stopped at the low signal-to-noise region of NUV frame, in which the small values of the radial intensity gradient induce the meaningless values for the ellipse parameters. The surface brightness measurements in the monochromatic system are given as μ_λ=−2.5logf_λ/A−21.1, where f_λ is the incidence flux in units of ergs s^{-1}cm^{-2}Å^{-1}, and A is the area of the ellipse in arcsec^{-2}.

(b) UV Surface Brightness and Color Distribution

Figure 1 shows the surface brightness profiles of the sample galaxies in NUV and FUV passbands. The profile of each galaxy is plotted as a function of the equivalent radius, which is defined by r = $\sqrt{ab}$, where a and b are the semi-major and semi-minor axis of the ellipse, respectively. Errors in surface brightness profiles are estimated from the root mean square scatter of the intensity data along the fitted ellipse. It is apparent that the surface brightness profiles follow a de Vaucouleurs law both in NUV and FUV passbands. From the simple concentric annuli surface photometry for the same galaxies, O'Connell et al. (1992) showed that the mean surface brightness profiles follow the de Vaucouleurs law, while some other early-type galaxies have their FUV profiles of the exponential function (Ohl et al. 1998). The general features of the NUV and FUV profiles of M31 and M81 are in agreement with the explanations of O'Connell et al. (1992). Our UV surface brightness profiles of M31 bulge extend to ~340". We note that Kent (1983, 1987) claimed the fraction of light contributed by the disk to the bulge profile inside 360" of M31 is negligible assuming the r$^{1/4}$ law describe the bulge profile. Our FUV surface brightness distribution of M32 is consistent with the profile of Ohl et al. (1998). NGC 1399 shows, however, a significantly different shape of the FUV profile in the region of r>30" in comparison with the result of O'Connell et al. (1992), i.e., $\Delta\mu$~1.0, while

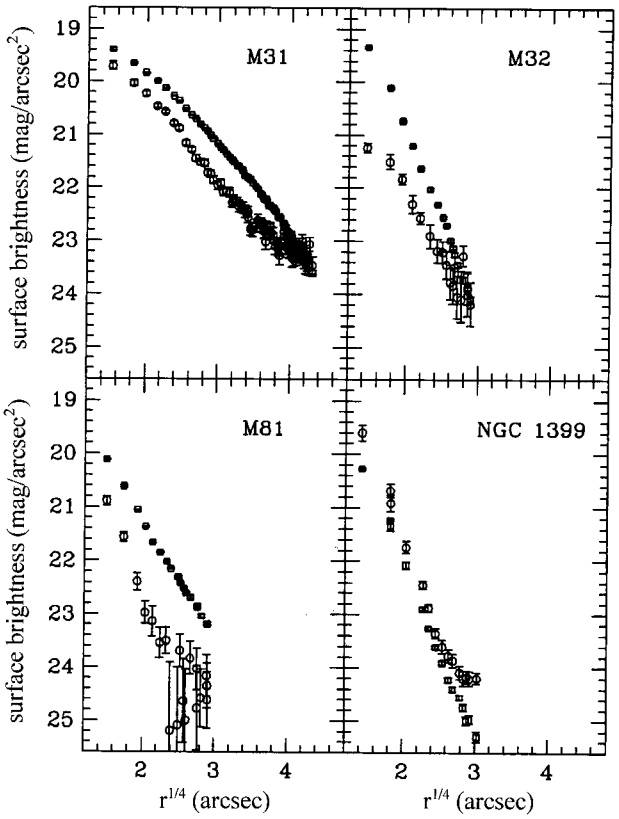

Fig. 1. NUV(square) and FUV(circle) surface brightness profiles of the sample galaxies, M31, M32, M81, and NGC 1399.

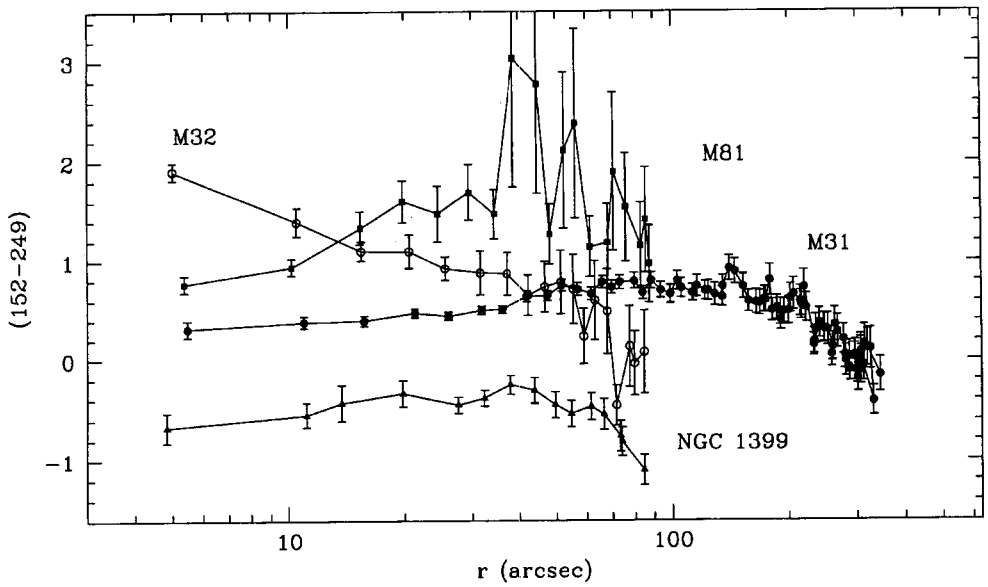

Fig. 2. FUV(1500 Å)-NUV(2490 Å) color distributions of the sample galaxies.

the NUV profiles are reasonably consistent each other. This result will affect the UV color distribution at the outer region of NGC 1399.

The UV colors defined by (152-249)=m_λ(1520 Å)-m_λ(2490 Å) in Figure 2. Because the extinction by internal dust is unlikely to be important in the UV color determination of the sample galaxies (O'Connell et al. 1992), no extinction correction is applied. It is apparent that the mean colors and color ranking of the galaxies in the central 20" region are in a good agreement with the results of O'Connell et al. (1992). We also confirmed the finding of O'Connell that the UV color becomes bluer as the galaxy is more luminous. Indeed, NGC 1399 is the most luminous one among the samples, while M32 is the faintest one. In the central regions of the three galaxies (M31, M81, and NGC 1399), the UV colors become bluer with decreasing radius. On the other hand, the color of M32 becomes redder toward the center.

The interesting feature of the UV color profiles in Figure 2 is that the radial UV color gradients are reversed in the outer parts of the three galaxies (i.e., M31, M81, and NGC 1399), in contrast to the inner regions. The UV color gradients become bluer outward in the outer parts of the color profiles of two spiral bulges; r>100" for M31 and r>40" for M81. NGC 1399 also has the same trend of the UV color gradient in the outer region r>40". As expected in the FUV surface brightness profile of NGC 1399 in Figure 1, the UV color distribution of NGC 1399 at outer region is significantly different to the result of O'Connell et al. (1992). These two-component trends in UV color profiles of these galaxies were not found in the previous study of O'Connell et al. (1992). Note that the outmost radii of their simple concentric annuli photometries were truncated at much smaller radii, i.e., r~100" for M31, r~50" for M81, and r~80" for NGC 1399, within which the UV color gradients of the three galaxies are still smooth in the sense of redder from the centers. On the other hand, the color gradient of M32 continuous to become bluer outward up to r~100". The UV color gradients of M32 found by O'Connell et al. (1992) and Ohl et al. (1998) also show a consistent trend to our result out to r~50".

(c) UV Isophote Shape Analysis

The radial variation of the ellipticity, ε, and the position angle, PA, of individual galaxies are presented in Figure 3 for the sample galaxies. The position angle was measured from the north towards the east. To compare the variations measured in other passbands, we also provide the ellipticity and position angle profiles measured in optical/near-IR passbands adopted from Kent (1983) for M31 in *r*-band, Peletier (1993) for M32 in *R*-band, Tenjes (1992) for M81 in *B*-band, Franx, Illingworth, & Heckman (1989) for NGC 1399 in *R*-band. Because the position angle variation data of M81 were not available in other passbands, we compared the position angle of the optical major axis provided by Feri et al. (1996) and plotted in Figure 3 as an arrow.

Several features in the profiles of Figure 3 are notable. The PA and ε change significantly in the inner regions of M31, M81, and NGC 1399. Remind that these galaxies show UVX gradients bluer inward in the inner region. These changes along with isophotal twists are considered as evidences of the triaxiality of stellar systems (Stark 1977). In the inner regions of these gal-

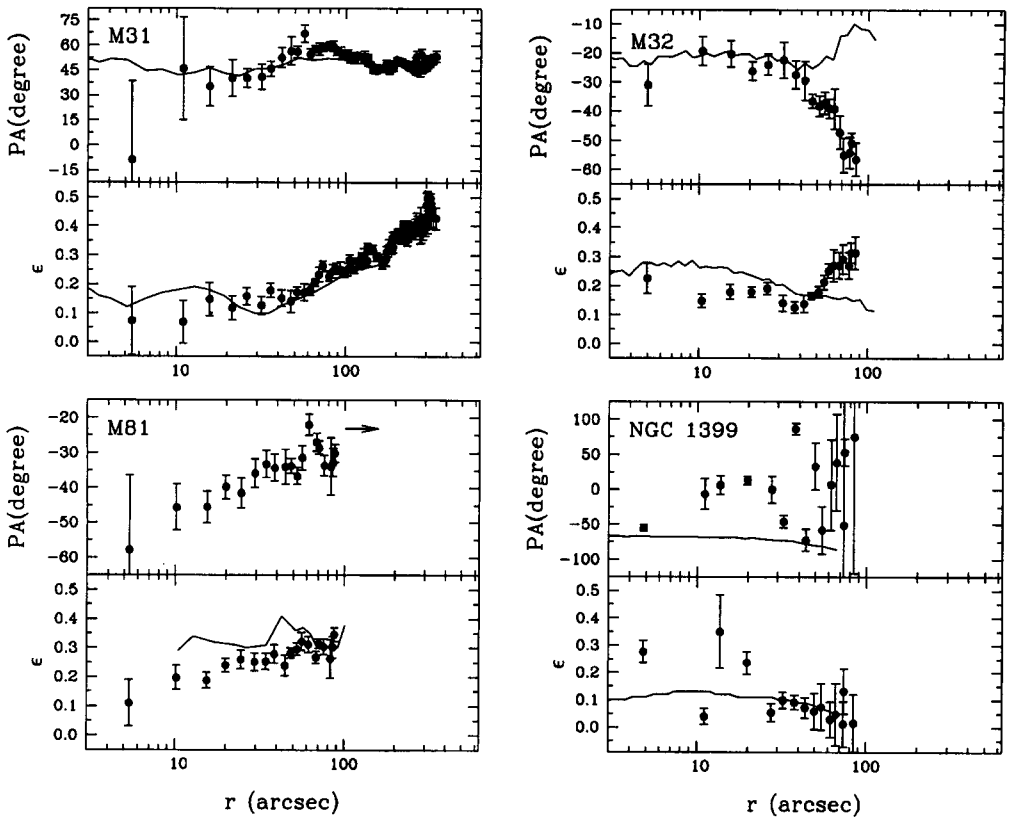

Fig. 3. The position angle (PA) and the ellipticity (ε) variations in the UV isophotes of the galaxies. Solid lines represent those in optical/near-IR passbands adopted from the previous studies.

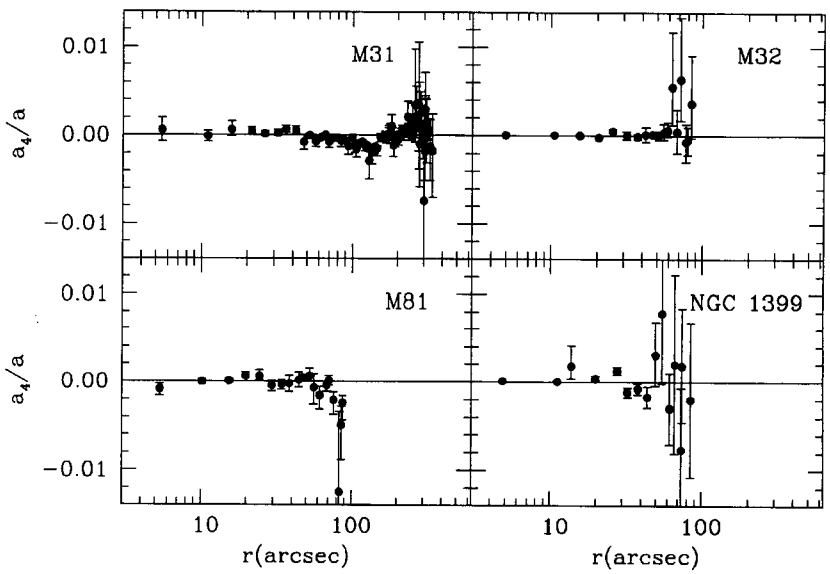

Fig. 4. Radial profiles of the fourth order Fourier coefficient $a(4)$ for the sample galaxies. We use the parameter $a(4)/a$, where a is the semi-major axis length of the corresponding isophote.

axies, the variations in the optical/near-IR passbands, however are much smaller than those in the UV. For case of M32, for which its UV image show reversed color gradient, the profile of PA and ε measured in UV passband are similar to that measured in *R*-band, and no significant radial variations are appeared throughout the inner region (r<50"). In the outer part of M32, however, there is a significant difference between the profiles measured in UV and *R*-band.

It is well known fact that the isophotes of a large fraction of elliptical galaxies show systematic deviations from pure ellipses (Jerdrzejewski 1987; Bender, Döbere-

iner, & Möllenhoff 1988; Bender et al. 1989; Milvang-Jensen & Jørgensen 1999). For most spheroidal galaxies, the dominating fourth order cosine coefficient $a(4)$ is generally used to distinguish between the boxy ($a(4)<0$) and disky ($a(4)>0$) shapes. From a magnitude-limited optical sample of northern elliptical galaxies, Bender et al. (1988) found that 80% of the galaxies show systematic deviations larger than 0.2% in units of the semi-major axis length. These deviations are examined to our sample galaxies by applying the Fourier transform to the azimuthal variations of the UV isophote.

The radial profiles of $a(4)$ are shown in Figure 4 for the sample galaxies. Here, we adopt the parameter $a(4)/a$, where a is the semi-major axis length of the corresponding isophote, rather than $a(4)$ itself in order to use the scale free parameter. The mean values of $a(4)/a$ for all four galaxies indicate that the systematic deviations of isophote are much smaller than $a(4)/a$~0.2%. Neither significant radial changes in $a(4)/a$ are shown in Figure 4 for the sample galaxies. These results indicate that the UV isophotes of the sample galaxies have pure elliptical shapes, i.e., neither boxy nor disky.

IV. DISCUSSION

In the previous section, we confirmed that the NUV and FUV lights of the nearby elliptical galaxies (M32, NGC 1399) and spiral bulges (M31, M81) are distributed smoothly, following the de Vaucouleurs law of the surface brightness profiles, indicating that there is no evidence of emissions by young and massive stars, i.e., clumps or knots, in these old stellar systems (cf. O'Connell et al. 1992). Also, the UV surface photometry, which has been applied by the ellipse fitting, delivered the evidence for the radial color gradients in UV of large amplitude in these sample galaxies. Three of them (M31, M81, and NGC 1399) show a two-component trend, in which the UV color becomes bluer inward through the inner regions and becomes bluer outward at the outer regions. For M32, however, the color continues to become bluer as the galactocentric distance increases.

The properties of the UV color distributions in the sample galaxies are very different from the behavior of early-type galaxies at optical/IR wavelengths (e.g., Peletier et al. 1990) as pointed by O'Connell et al. (1992). Note that early-type galaxies with old stellar populations typically exhibit remarkably homogeneous color and have a small color gradient in the optical passband, and the optical colors of more luminous galaxies are slightly redder. This leads the fact that the two-component structure in the UV color profiles in Figure 2 is a distinct behavior for the UVX phenomena. Ohl et al. (1998) found the breaks in the FUV-B color slopes of seven early-type galaxies, i.e., the inner plateau and a steep reddening outward, which are not common in optical gradient, either. The radial UV color distribution of M32 is also very important because there is evidence of intermediate age (<8 Gyr) population and the radial age gradient in M32 (O'Connell 1999, and references therein). Peletier (1993) claimed, however, that the metallicity and the age of the outer region (up to r=30") of M32 are not different from those of the center, since all optical and infrared colors, as well as the infrared CO bands are constant in M32 as a function of radius, and since there is no evidence of the absorption line gradients such as in Mg_2 (Davidge 1991).

The position angle and the ellipticity variations on the isophote represent the dynamical structure of the system. The position angle profiles are used to estimate the isophote twist, which is direct evidence of the triaxiality of the system. The mean ellipticity of the boxy ellipticals tends to be smaller than ellipticals with purely elliptical isophote in optical passband (Bender et al. 1989). For M31, M81, and NGC 1399 in which remarkable radial UV color gradients exist in the sense bluer inward through the inner region, the position angle and the ellipticity in UV images vary significantly through the inner region as shown in Figure 3, while those in the optical/near-IR do not show a significant variation. Similar results were drawn by Reichen et al. (1994) from the investigation of the UV image of M81. They found that the ellipticity decreased from 0.33 at a=50" to 0.28 at a=30". They also confirmed that these variations are not simply artifacts of nonuniform extinction. We therefore suggest that the radial UVX in early-type galaxies and spiral bulges has been influenced by the dynamical structure of the UVX populations. In addition, the different distributions in the position angle and ellipticity in UV and optical/IR isophotes indicates three dimensional distribution of the UV population must differ from that of the optical population.

In case of M32, there are significant variations of the position angle and ellipticity in the outer part. This feature is not the same in the case of the giant elliptical galaxy NGC 1399 in our sample. M32 is tidally truncated by interaction with neighboring M31. Moreover, M32 is classified as a compact elliptical galaxy, while NGC 1399 is a giant elliptical galaxy. It has been thought that compact elliptical galaxies are the remnants of ellipticals or spirals after a tidal interaction with a much larger galaxy. Also, the optical/IR color gradients in compact and dwarf ellipticals are different from those of giant elliptical galaxies (Peletier 1993). Therefore, tidal interaction with the massive companion galaxy M31 may have had strong effects on the dynamical structure of M32, and then the spatial distribution of the UVX

populations.

There has been some evidences that the emission in UV and optical passbands of early-type galaxies is correlated to the shape of their isophotes, i.e., boxy or disky shapes. As noted in the introduction, Longo et al. (1989) presented a correlation between the isophote shape parameter a_4/a and the UV color index; boxy galaxies are found to be UV brighter than disky galaxies. Peletier et al. (1990) also found a similar tendency that the more boxy shape of the isophote, the smaller color gradients in *B-R* and in *U-R*. In this paper, however, we could not find any strong evidence supporting the correlation between the UV color gradient and the isophotal shapes. Note that deviations for the boxy or disky shapes are common at 1% level as presented by several authors (e.g., Bender et al. 1988; Peletier et al. 1990). As shown in Figure 4, however, the UV isophotes of the sample galaxies are close to pure ellipse with the small value of the fourth order cosine coefficients, i.e., $|a(4)/a|<0.002$, rather than boxy or disky shape, although there was evidence that the shape of the M31 bulge is boxy in the *r*-band isophotes (Kent 1983, 1987). Moreover, no significant radial change of $a(4)/a$ is shown in Figure 4.

The UV flux of a galaxy can be affected by several other facts. The main interpretation of the UV color variations in elliptical galaxies and the spiral bulges includes the metal ablundance and age differences of the stellar components. Burstein et al. (1988) found that the more metal-rich nuclei as measured by the Mg_2 index have stronger UVX components. In a galaxy, the UVX would become stronger inward, as metal abundance increases inward. This sense of the correlation between the radial UVX and abundance distribution is the same as the overall UVX/abundance correlation of Burstein et al. (1988). By contrast, Ohl et al. (1998) found no correlation between the metallicity gradient and the radial UVX gradients. This implies that the UVX may not be simply related to the metal abundance. The UV emission is sensitive to change in the age of the population as well, i.e., the UVX increases as the HB envelope mass decreases with increasing age. Indeed, Lee (1993, 1994) pointed out that the apparent correlation between the UVX and Mg_2 metallicity index based on the optical spectra of elliptical galaxies (Burstein et al. 1988) may not be the only evidence that the UV light itself is originated from the metal-rich population. Instead, he attributed the UV lights to the age spread of hot and old horizontal branch population. Park & Lee (1997) interpreted the UVX as the product of a metal poor subpopulation of extremely old stars with ages of about 3 Gyrs older than the Galactic halo population. They also suggested that the UVX variation within a galaxy and its correlation with the observed line strength is caused by the variation in age, with the stronger UVX being older. The UV light, however, is suffered from an age-abundance degeneracy (e.g., Yi et al. 1999) in elliptical galaxies and spiral bulges which contain a stellar component with an effective temperature higher than 20,000 K that appears to be unusually sensitive to the age and chemical abundance of their old populations. Properties, such as, mass loss processes on the RGB and the helium abundance of the UVX populations may also affect the UV output in a galaxy, coupled with the metallicity and the age (O'Connell 1999).

Despite of the recent intensive studies of the UVX phenomenon, the interpretation of the UVX phenomena in elliptical galaxies and the spiral bulges is still controversial mainly due to the lack of observational data. Moreover, their UV photometric properties derived from the UIT data still include uncorrected background subtraction errors induced by the plate fog of the photographic detector as mentioned in §3. The UV imaging/spectroscopic data from the GALEX mission (Martin et al. 1997), which are now under developing to launch in 2002, could be used to understand more confidently the feature of the UVX within and among the elliptical galaxies and the spiral bulges.

V. SUMMARY

The correlation between the radial UV color distribution and the shapes of the UV isophote has been investigated by applying the ellipse fitting technique to the isophotes of the archival *UIT* images of four nearby elliptical galaxies and spiral bulges. From the results of ellipse fitting to the *UIT* images, we presented the detailed photometric and morphological properties of the galaxies, i.e., the radial surface brightness profiles in the UV, radial color distributions in (1520-2490 Å), and the isophote shape parameter variations of the position angle, the ellipticity, and $a(4)/a$.

The UV surface brightness profiles of the galaxies followed the de Vaucouleurs law with no evidence of emissions by young and massive stars. There is a two-component trend in the radial UV color distribution of the giant elliptical galaxy NGC 1399 and two bulges of the nearby spiral galaxies M31 and M81, in the sense of bluer inward in the inner region and bluer outward in the outer region. The color gradient of M32 became continuously bluer to the larger radii. The position angle and the ellipticity in UV isophotes of M31, M81, and NGC 1399, varied significantly through the inner regions showing the triaxiality of the systems. M32 showed, however, significant variations in position angle and ellipticity at the outer region of the UV isophote. These results suggest that the radial UVX distributions in early-type galaxies and spiral bulges may have a corre-

lation to the dynamical structure of UVX populations. However, the shape parameter $a(4)/a$, which is positive in disky galaxy and negative in boxy galaxy, indicated all the UV isophotes of the sample galaxies has a pure elliptical shape rather than the boxy or disky shapes.

This work is supported by the Creative Research Initiative Program of the Korean Ministry of Science and Technology.

REFERENCES

Bender, R. 1988, A&A, 202, L5
Bender, R., Döbereiner, S., & Möllenhoff, C. 1988, A&AS, 74, 385
Bender, R. & Möllenhoff, C. 1987, A&A, 177, 71
Bender, R., Surma, P., Döbereiner, S., Möllenhoff, C., & Madejsky, R. 1989, A&A, 217, 35
Binney, J.J. & Petruo, M. 1985, MNRAS, 214, 449
Burstein, D., Bertola, F., Buson, L.M., Faber, S.M., & Lauer, T.R. 1988, ApJ, 328, 440
Busko, I. 1996, in Astronomical Data Analysis Software and Systems V, ASP Conf. Ser. 101, Eds. G.H. Jacoby & J. Barnes (San Fransisco: ASP), 139
Chiosi, C. 1996, in From Stars to Galaxies: The Impact of Stellar Physics on Galaxy Evolution, ASP Conf. Ser. 98, Eds. C. Leitherer, U. F. Alvensleben, & J. Huchra (San Fransisco: ASP), 181
Code, A.D. 1969, PASP, 81, 475
Code, A.D. & Welch, G.A. 1979, ApJ, 228, 95
Davidge, T.J. 1991, Aj, 101, 884
Dorman, B., O'Connell, R.W., & Rood, R.T. 1995, ApJ, 442, 105
Feri, Z., Guhathakurta, P., Gunn, J., & Tyson, J.A. 1996, AJ, 111, 174
Franx, M., Illingworth, G., & Heckman, T. 1989, AJ, 98, 538
Greggio, L. & Renzini, A. 1990, ApJ, 364, 35
Hill, J.K. et al. 1993, ApJ, 402, L45
Jedrzejewski, R. I. 1987, MNRAS, 226, 247
Kent, S.M. 1983, ApJ, 266, 562
Kent, S.M. 1987, AJ, 94, 306
Kuchinski et al. 2000, astro-ph/0002111
Lee, Y.-W. 1993, in The Globular Cluster-Galaxy Connection, ASP Conf. Ser. 48, Eds. G.H. Smith, & J.P. Brodie (San Fransisco: ASP), 142
Lee, Y.-W. 1994, ApJ, 430, L113
Longo, G., Capaccioli, M., Bender, R. & Busarello, G. 1989, A&A, 225, L17
Martin, C. et al. 1997, BAAS, 191, #63.04
May, A. van Albada, T.S., & Norman, C.A. 1985, MNRAS, 214, 131
Milvang-Jensen, B. & Jørgensen, I. 1999, Baltic Astronomy, 8, 535
Nieto, J.-L. 1989, Astronomia Extragalactica, Academia Nacional de Ciencias de Cordoba, 239
O'Connell, R.W. 1999, ARA&A, 37, 603
O'Connell, R.W. et al. 1992, ApJ, 395, L45
Ohl, R.G. et al. 1998, ApJ, 505, L11
Park, J.-H. & Lee, Y.-W. 1997, ApJ, 476, 28
Peletier, R.F. 1993, A&A, 271, 51
Peletier, R.F., Davies, R.L., Illingworth, G., Davies, L., & Cawson, M. 1990, A&AS, 100, 1091
Reichen, M., Kaufman, M., Blecha, A., Golay, M., & Huguenin, D. 1994, A&AS, 106, 523
Stark, A.A. 1977, ApJ, 218, 368
Stecher T.P. et al. 1992, ApJ, 395, 1
Stecher T.P. et al. 1997, PASP, 109, 584
Tenjes, P. 1992, Baltic Astronomy, 1, 7
Yi, S., Demarque, P., & Oemler, A. 1997, ApJ, 486, 201
Yi, S., Lee, Y.-W., Woo, J.-H., Park, J.-H., Demarque, P., & Oemler, A. 1999, ApJ, 513, 128